Assimilation of Synthetic Remotely Sensed Soil Moisture in Environment Canada's MESH Model

Xiaoyong Xu, Bryan A. Tolson, Jonathan Li, *Senior Member, IEEE*, and Bruce Davison

***Abstract*—With recent advances in satellite microwave soil moisture estimation, particularly the launch of the Soil Moisture and Ocean Salinity satellite and the soil moisture active passive mission, there is an increased demand for exploiting the potential of satellite microwave soil moisture observations to improve the predictive capability of hydrologic and land surface models. This study presents the implementation of the 1-D version of the ensemble Kalman filter scheme to assimilate satellite soil moisture into Environment Canada's Standalone Modélisation Environmentale-Surface et Hydrologie (MESH) model that couples the Canadian land surface scheme with a distributed hydrological model. This paper examines the performance of the established assimilation scheme by conducting a series of synthetic assimilation experiments in which the satellite soil moisture and the reference ("true") solutions were derived from the MESH model simulations. The synthetic analyses have demonstrated the capability of the assimilation system, given the synthetic satellite soil moisture and the intentionally degraded model estimates, to accurately approximate the "true" surface layer and root-zone soil moisture solutions. The experiments have also revealed the impacts of a series of factors (ensemble size, vegetation cover, observing frequency, specification of observation, and model input error parameters) upon the quality of the assimilation estimates, which can provide an important guidance for the practical application of the assimilation scheme.**

***Index Terms*—Data assimilation, ensemble Kalman filter (EnKF), Modélisation Environmentale-Surface et Hydrologie (MESH), satellite soil moisture, synthetic experiment.**

I. Introduction

OVER the past decades, the global water cycle has suffered from increasing uncertainties introduced by climate change, land use, and human activities, which in turn added pressure on management of water resources. Soil moisture is one of the most important parameters to characterize the water cycle behavior and water resources availability. Soil moisture, as a key state variable linking the land surface and the atmosphere, can bring a significant component of memory into the soil-atmosphere system through an integration of precipitation and evaporation processes over time scales of days to months. The memory has an important influence on surface saturation, precipitation, runoff, and forecasting of flooding events [1]—[3]. As a reservoir for evapotranspiration, soil moisture also has an important controlling on the partitioning of energy fluxes between latent and sensible forms at the land surface, which could considerably modulate the large-scale atmospheric circulation and temperature patterns during summers [4], [5].

Traditionally, soil moisture can be *in situ* measured using a gravimetric method or ground-based sensors. *In situ* measurements typically serve as the "ground truth," but spatially distributed soil moisture information, especially at regional, continental, or global scales, is difficult to estimate from *in situ* measurements, which are typically based upon sparse point sources in practice. Satellite microwave remote sensing (e.g., [6]–[11]) holds the ability to provide large-scale monitoring of surface soil moisture because microwave measurements respond to changes in the surface soil's dielectric properties, which are strongly controlled by soil water content. However, although satellite microwave soil moisture observations, relative to ground-based point measurements, have better geographical coverage and can contribute to many fields (e.g., [12]–[14]), satellite remote sensing cannot directly produce spatiotemporally complete soil moisture estimates that are typically required in many practical applications (e.g., initialization of weather and hydrological models) [15]. For a given location, the revisiting time of a satellite sensor system is typically 1–3 days (separately for ascending and descending orbits) or much longer depending upon the satellite sensor system and the latitude. Additionally, satellite remote sensing cannot directly measure soil water content below a surface layer. Therefore, to produce spatiotemporally complete soil moisture estimates, we need to spread satellite observed information to times and locations that are not directly measured by satellite sensors.

On the other hand, land surface and hydrological model simulations, in particular, for physically based distributed models, allow for the estimation and prediction of hydrologic conditions at desired spatial and temporal scales. In practice, however, land surface and hydrologic modeling is often difficult because we have neither a perfect forecast model nor perfect meteorological forcing data, i.e., the accuracy of state estimation suffers from uncertainties in forcing fields and deficiencies in model physics and/or parameters. To improve the model simulations, one may constrain the model forecasted state in time with observations. To what extent the model forecast will be modified given ob-

Manuscript received June 24, 2016; revised October 8, 2016; accepted October 27, 2016. Date of publication December 4, 2016; date of current version March 22, 2017. This work was supported in part by a NSERC CGSD and a Meteorological Service of Canada Graduate Supplement. *(Corresponding author: Jonathan Li.)*

X. Xu and J. Li are with the Department of Geography and Environmental Management, University of Waterloo, Waterloo, ON N2L 3G1, Canada (e-mail: xiaoyong.xu@uwaterloo.ca; junli@uwaterloo.ca).

B. A. Tolson is with the Department of Civil and Environmental Engineering, University of Waterloo, Waterloo, ON N2L 3G1, Canada (e-mail: btolson@uwaterloo.ca).

B. Davison is with the National Hydrology Research Centre, Environment Canada, Saskatoon, SK S7N 5A2, Canada (e-mail: bruce.davison@ec.gc.ca).

Color versions of one or more of the figures in this paper are available online at http://ieeexplore.ieee.org.

Digital Object Identifier 10.1109/JSTARS.2016.2626256

servations is controlled by the model forecast and observation error covariances. Meanwhile, the observed information can, by means of consistency constraints based upon the time evolution and physical properties of the system, spread to times and locations that are not directly observed. This is the basic concept of data assimilation.

There has been an intensive global research effort to assimilate microwave remote–sensing soil moisture into land surface or hydrological models over the past few decades [16]. The studies have demonstrated the potential of remotely sensed soil moisture, through data assimilation, to improve the predictive capability of hydrologic and land surface models. However, the relevant efforts have to date been focused upon assimilation of remotely sensed soil moisture in catchment scale [17]–[20], coarse scale [21], or lumped models [22], [23]. Here, we equip Environment Canada's Standalone Modélisation Environmentale-Surface et Hydrologie (MESH), which is a distributed land surface-hydrological model [24], with a satellite soil moisture data assimilation scheme. The assimilation of satellite soil moisture retrievals will be conducted at a grid scale that is comparable to practical satellite product scales.

This paper examines the performance of the established assimilation scheme for the MESH model by conducting a series of synthetic assimilation experiments. The satellite soil moisture data were derived from the forecast model MESH simulations, and the reference ("true") solutions are known. This allows investigation of the impacts of a series of factors (ensemble size, vegetation cover, observing frequency, specification of observation, and model input error parameters) upon the quality of the assimilation estimates, which can provide a basis for the practical application of the assimilation scheme. This paper is organized as follows. In Section II, the forecast model is introduced. Section III describes the data assimilation scheme. The synthetic experiment setup and results are presented in Section IV, followed by a summary and discussion in Section V.

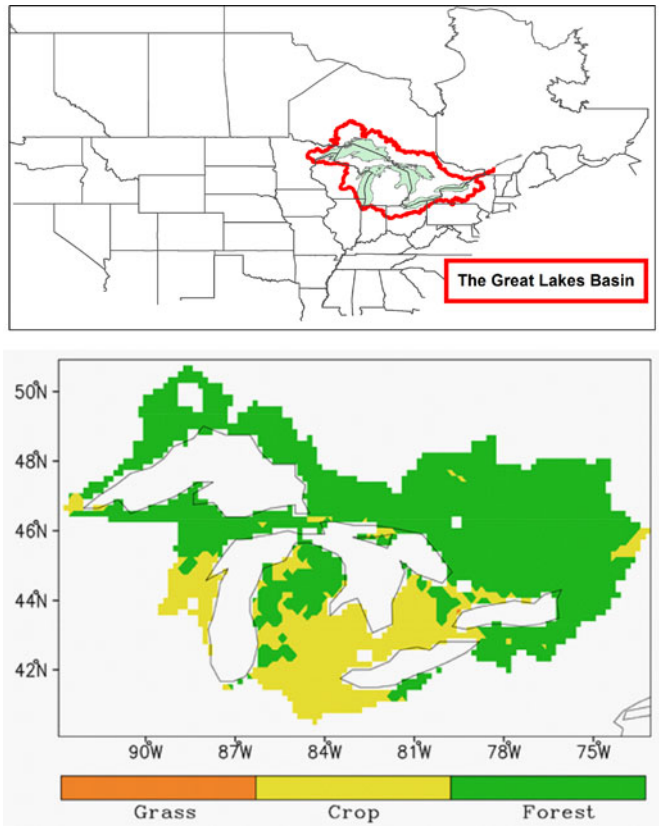

Fig. 1. Great Lakes basin and its land cover. Note that each grid cell (1/6th of a degree resolution) may consist of a maximum of seven land cover classes (crop, grass, deciduous forest, coniferous forest, mixed forest, water, and impervious). Only the dominant land over class is displayed for each grid here (a forest cover represents the sum of the deciduous, coniferous, and mixed forest classes). Water and impervious surfaces are not labeled since soil moisture estimates are not evaluated for them.

II. Model and Experimental Domain

Environment Canada's standalone MESH is a land surface and hydrological model in which the Canadian land surface scheme (CLASS) is coupled with a hydrological routing model WATFLOOD [24]. A primary innovation of MESH is that the model uses a grouped response unit (GRU) approach [25] to resolve the heterogeneity in geophysical fields. A GRU is a grouping of subareas with similar soil and/or vegetation attributes. In the version of MESH used in this study, each GRU corresponds to one land cover class (other soil characteristics are assumed to be same for the same GRU). Each model grid cell is represented by a limited number of distinct GRUs (tiles) weighted by their respective cell fractions. It is acknowledged that the current GRU scheme, which is based solely on land cover, is still not sufficient to resolve the basin heterogeneity. To better meet the requirements for many practical applications, other physiographic features, such as soil type, erosion, topography, and slope (e.g., [26]–[28]) also need to be taken into account in the GRU definition, although this is outside the scope of this study and may be considered in the future efforts to improve the MESH model system.

The land model is run on each tile independently. The overall fluxes and prognostic variables of a grid cell are obtained by taking a weighted average of the results from tiles. The soil column is partitioned into three layers (0–10, 10–35, and 35–410 cm) to resolve water and temperature dynamics. In practice, satellite microwave sensors measure only the water content within the top few centimeters of soil, which approximately matches with the model surface layer. The land surface scheme considers only the vertical water movement between the soil layers, which is governed by the 1-D Richard's equation

$$\partial\theta/\partial t = -\partial K(\theta)/\partial z + \partial\left(K(\theta)\left(\partial\psi(\theta)/\partial z\right)\right)/\partial z \quad (1)$$

where θ denotes the volumetric water content, t is the time, z is the depth of soil, $K(\theta)$ is the hydraulic conductivity, and $\psi(\theta)$ is the pressure head (soil water suction). The lateral movement of water between grids/tiles is not taken into account. The resulting horizontal flows (overland flow, interflow, and base flow) within grid cells are ultimately routed into the stream and river network systems.

The experimental domain is the Great Lakes basin (see Fig. 1). The MESH model has been applied to this basin before [24],

[29]. The corresponding model configurations [24] and calibrated parameters [29] can be directly used in this study. Seven GRU types are identified for this domain: crop, grass, deciduous forest, coniferous forest, mixed forest, water, and impervious. Each GRU class has a different model parameter set. The basin is gridded at ten arcmins ($\sim$15 km $\times$ 15 km) in the model simulations. Each model grid is a mosaic of the seven GRU classes weighted by their cell fractions.

III. Data Assimilation Scheme

In a data assimilation system, the observed information is integrated into the model framework by taking into account both the model forecast and observation error characteristics. This allows the model forecast and observation to be optimally merged, while without violating the model physical constraints. Here, we use the ensemble Kalman filter (EnKF) scheme to assimilate satellite soil moisture into the MESH model. The EnKF method is chosen because 1) as compared to the variational methods, the EnKF is relatively easy to implement since an adjoint version (a conjugate transpose of the tangent linear model) of the forecast model is not required; 2) estimation of full error covariances is not required, and the model and measurement error variances are defined by the ensemble spreading (although the input error parameters need to be specified or to be adaptively tuned); and 3) EnKF is an ensemble-based method, and, thus, can be easily merged into the existing ensemble forecasting system in use with Environment Canada.

The EnKF, which was first introduced by [30], uses a Monte–Carlo approach to estimate the forecast and observation error statistics. An ensemble of model states is used to approximate the probability density of the model state. The ensemble spread defines the forecast error variance and the ensemble mean is considered as the best estimate (Gaussian assumption). Thus, the error covariance equation (as used in the Kalman filer or the extended Kalman filter) for the evolution of the model forecast error information can be replaced by integrating the ensemble of model states forward in time, expressed as

$$x^{-}_{j,\,t} = M\left(x^{+}_{j,\,t-1}, u_{j,t}\right) \tag{2}$$

where M denotes the forecast model operator, $x^{+}_{j,t-1}$ represents a posterior (analysis) model state at measurement time $t-1$. $x^{-}_{(j,t)}x^{f}_{j}$ is *a priori* (forecast) model state at measurement time t. $u_{j,t}$ denotes the model uncertainties (perturbations to the forcing data and deficiencies in model parameters/physics). The subscript j is the ensemble member index, counting from 1 to the size of the ensemble N. The observation is perturbed to generate an ensemble of perturbed observations with the ensemble mean equal to the actual observation and the spreading of the ensemble as the observation error variance, i.e.,

$$y_{j,t} = \bar{y}_t + \varepsilon_{j,t} \tag{3}$$

$$R_t = (N-1)^{-1}\sum_{j=1}^{N}\varepsilon_{j,\,t}\,\varepsilon^{T}_{j,\,t} \tag{4}$$

where $\bar{y}_t$ and $y_{j,t}$ represent the actual observation and the perturbed observation at time t, respectively. $\varepsilon_{j,\,t}$ and R_t denote the observation error perturbation and the observation error covariance, respectively. The superscript T denotes the vector transpose. At measurement time t, each of the model forecast state ensemble members $x^{-}_{j,\,t}$ is updated to $x^{+}_{j,\,t}$ according to the Kalman analysis equation, given by

$$x^{+}_{j,\,t} = x^{-}_{j,\,t} + P^{-}_{t}H^{T}_{t}\left(H_t P^{-}_{t} H^{T}_{t} + R_t\right)^{-1}\left(y_{j,t} - H_t x^{-}_{j,t}\right) \tag{5}$$

where H_t is the measurement operator. P^{-}_{t} denotes the forecast error covariance. In the EnKF, P^{-}_{t} is only implicitly needed through

$$P^{-}_{t}H^{T}_{t} = (N-1)^{-1}\sum_{j=1}^{N}\left[\left(x^{-}_{j,\,t} - N^{-1}\sum_{j=1}^{N}x^{-}_{j,\,t}\right)\left(H_t x^{-}_{j,\,t} - N^{-1}\sum_{j=1}^{N}H_t x^{-}_{j,\,t}\right)^{T}\right] \tag{6}$$

$$H_t P^{-}_{t} H^{T}_{t} = (N-1)^{-1}\sum_{j=1}^{N}\left[\left(H_t x^{-}_{j,\,t} - N^{-1}\sum_{j=1}^{N}H_t x^{-}_{j,\,t}\right)\left(H_t x^{-}_{j,\,t} - N^{-1}\sum_{j=1}^{N}H_t x^{-}_{j,\,t}\right)^{T}\right]. \tag{7}$$

Ultimately, through conducting in turn the forecast step, as in (2), and the update step, as in (5), the observational information is sequentially accumulated into the model state. Considering that the MESH model grid cells are modeled as independent soil columns in the land scheme (see Section II), the 1D-EnKF where the horizontal correlations between the model grids are neglected and an observation influences only the model state at the observation location is used here.

In this study, the model state vector x, which has a dimension of 21 and is independent for each grid, is comprised of the volumetric water content from the seven GRUs (tiles) for the model's three soil layers. The observation y_j is the perturbed satellite retrievals of surface soil moisture, and the corresponding model prediction Hx^{-}_{j} denotes the volumetric liquid water content (a weighted sum of GRUs within the grid) in the model surface layer. In the assimilation, the updating of the model soil moisture estimates, as in (5), is applied only to the five vegetation GRUs (i.e., crop, grass, deciduous forest, coniferous forest, and mixed forest). The state updating is not considered for water and impervious surface GRUs. A model grid cell, if the fraction of water or impervious surface GRU exceeds 5%, is excluded from the soil moisture evaluation and assimilation. The state updating is conducted for all the three soil layers of MESH. However, to be consistent with real application, we do not assess the model and assimilation estimates of soil water content for the third soil layer (i.e., from 35 cm below the surface to the water table) since *in situ* soil moisture measurements at those depths are very sparse in our study basin.

TABLE I
LIST OF SYNTHETIC EXPERIMENTS

Key	Description
A	Control experiment; Ensemble size $N = 12$; Assimilation interval is 24 h
B1	Same as A, but with $N = 6$
B2	Same as A, but with $N = 50$
B3	Same as A, but with $N = 100$
C1	Same as A, but with assimilation interval of 12 h
C2	Same as A, but with assimilation interval of 72 h
D1	Same as A, except for a higher retrieval skill
D2	Same as A, except for a lower retrieval skill
E1–E25	Test the impact of the specified model and observation input error parameters

IV. EXPERIMENT SETUP AND RESULTS

The synthetic experiments are designed as follows. First, the MESH model is integrated for one-year period (1 January to 31 December) using the meteorological forcings derived from the Global Environmental Multiscale (GEM) model [31] forecasts of year 2005. Each GRU class has its own model parameter set, which was based upon a global calibration with streamflow observations [29]. The model integration is spun up with the GEM forcings of year 2004 (repeatedly for ten year). The simulated soil moisture serves as the reference solution ("truth"). The synthetic satellite soil moisture retrievals are generated, independently for each model grid, by applying the random Gaussian white noise (the error standard deviation is set to $0.08\,\mathrm{m^3/m^3}$) to the true surface soil moisture sequence. Next, we perform an open-loop model simulation (without data assimilation), which intentionally deviates from the true integration. To this end, the MESH model is integrated for one-year period again but with the GEM forcings of year 2006 and using a different set of model parameters, which are generated by adding random noise with a standard deviation of 30% (of magnitude) to the model parameters used in the true integration. Finally, the synthetic soil moisture retrievals are assimilated into the open-loop integration, under different conditions, to examine the capability of the assimilation system to recover the "true" soil moisture solution. The assimilation experiments are listed in Table I. More details on the experiments will be provided in the remainder of this section.

This study examines the contribution of satellite soil moisture, through data assimilation, upon the model soil moisture estimates only. The effects of satellite soil moisture assimilation on other model variables (streamflow, evapotranspiration, surface heat fluxes, etc.) are outside the scope of this study since estimates of those variables are sensitive to the input error parameters [32]. The period 2004–2006 was chosen because the model parameter set (associated with physiography, vegetation, and soil characteristics) was based upon a calibration to the 2004–2005 streamflow observations [29].

A. Control Experiment

Experiment A is a control case that uses the 1D-EnKF with 12 ensemble members. The EnKF method estimates the model forecast errors based upon an ensemble of model integrations.

TABLE II
ERROR PARAMETERS FOR THE SELECTED FORCING INPUTS AND MODEL VARIABLES

	Perturbation Method[a]	Standard Deviation	Temporal Correlation	Cross Correlation[b]
Forcing inputs[c]				
Precipitation (P)	M	0.5	1 day	−0.8 with SW 0.5 with LW
Incoming shortwave radiation (SW)	M	0.2	1 day	−0.8 with P −0.5 with LW
Incoming longwave radiation (LW)	A	$40\,\mathrm{W\,m^{-2}}$	1 day	0.5 with P −0.5 with SW
Volumetric liquid water				
First soil layer	A	$1.0\mathrm{E}-03\,\mathrm{m^3\,m^{-3}}$	1 day	n/a
Second soil layer	A	$5.0\mathrm{E}-04\,\mathrm{m^3\,m^{-3}}$	1 day	n/a
Third soil layer	A	$5.0\mathrm{E}-05\,\mathrm{m^3\,m^{-3}}$	1 day	n/a

[a]Perturbation method: Multiplicative (M) or additive (A).
[b]The cross-correlated perturbations in precipitation and radiation fields were generated following [18] to represent an equilibrium state between them.
[c]Error parameters for the selected forcing inputs are adapted from [18].

The cross-correlated forcing perturbation fields, which were generated following [18], are applied to meteorological forcing fields of precipitation and radiation (see Table II) to represent random errors in these fields and an equilibrium state between them. The random errors in the forcing data typically vary with time and space and are difficult to completely quantify. The perturbation values used here were mainly based upon order-of-magnitude considerations (i.e., the mean error behavior for GEM forecasts).

To account for the model uncertainties due to imperfect model parameters, temporally correlated error perturbations are added to the forecasted volumetric liquid water content (see Table II). The specified model input error parameters are derived from the filter calibration experiment (not shown). A true observation error standard deviation of $0.08\,\mathrm{m^3/m^3}$ is used for the synthetic retrievals (recall that the synthetic retrievals are generated by adding the Gaussian white noise with standard deviation of $0.08\,\mathrm{m^3/m^3}$ to the true surface soil moisture). The assimilation is performed at 24-h intervals (i.e., we assume the observing frequency of once daily). The satellite retrieval-model discrepancies in climatological mean and spatial scale are not present, and, thus, not considered in our twin experiments.

Fig. 2 shows the open-loop model (without assimilation) and the assimilation surface (0–10 cm) soil moisture estimates across the study domain, in comparison with the "true" state. The assimilation estimates show, relative to open loop, better overall agreement with the true fields in terms of the distribution and magnitude of soil moisture across the study domain. This demonstrates that the EnKF scheme installed for the MESH model can be effective to improve the model surface soil moisture estimates. The counterpart of Fig. 2 for root-zone (0–35 cm) soil moisture is provided in Fig. 3. The root-zone soil moisture estimates are also improved through the assimilation of the surface soil moisture retrievals. The successful updating of root-zone soil moisture indicates that through data assimilation, the near-surface soil moisture information, which can be acquired

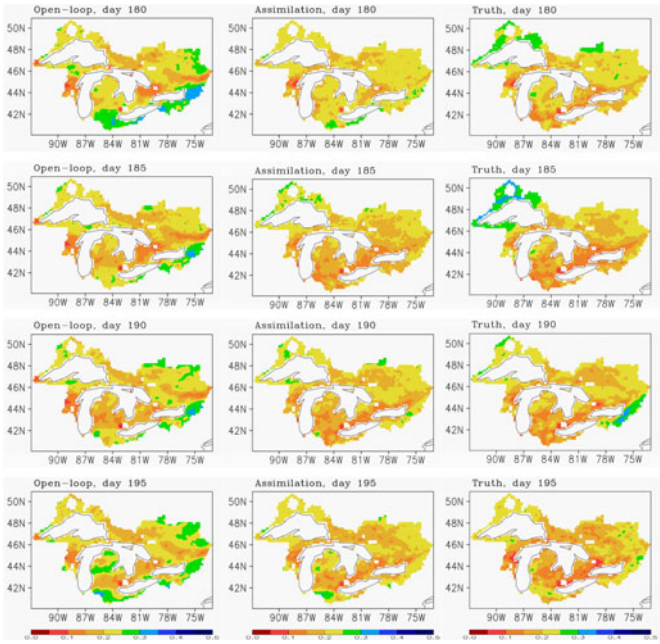

Fig. 2. Daily averaged surface (top 10 cm) soil moisture estimates (m^3m^{-3}) from (left) the open-loop model (middle), the assimilation, and (right) the true state for (top to bottom) days 180, 185, 190, and 195, respectively.

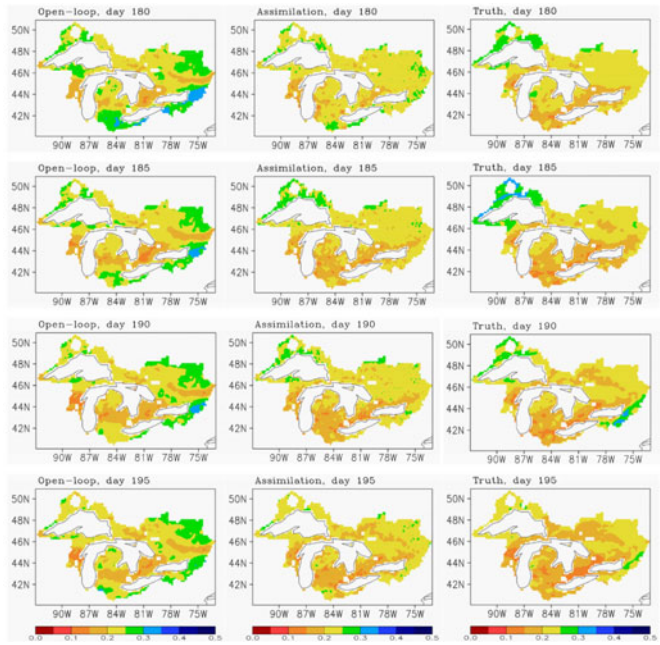

Fig. 3. Similar to Fig. 2, but for root-zone (top 35 cm) soil moisture, which is a depth-weighted average of soil moisture in the model's top two layers (0–10 and 10–35 cm).

by satellite microwave remote sensing, can spread to deeper soil layers that are not directly measured by satellite sensors. Note that an efficient constraint of satellite retrievals on root-zone soil moisture relies upon the model's accurate description of water movement in the soil column. In our twin experiment, the model physics is satisfactorily represented since we used the same model (but different model parameters) to generate the

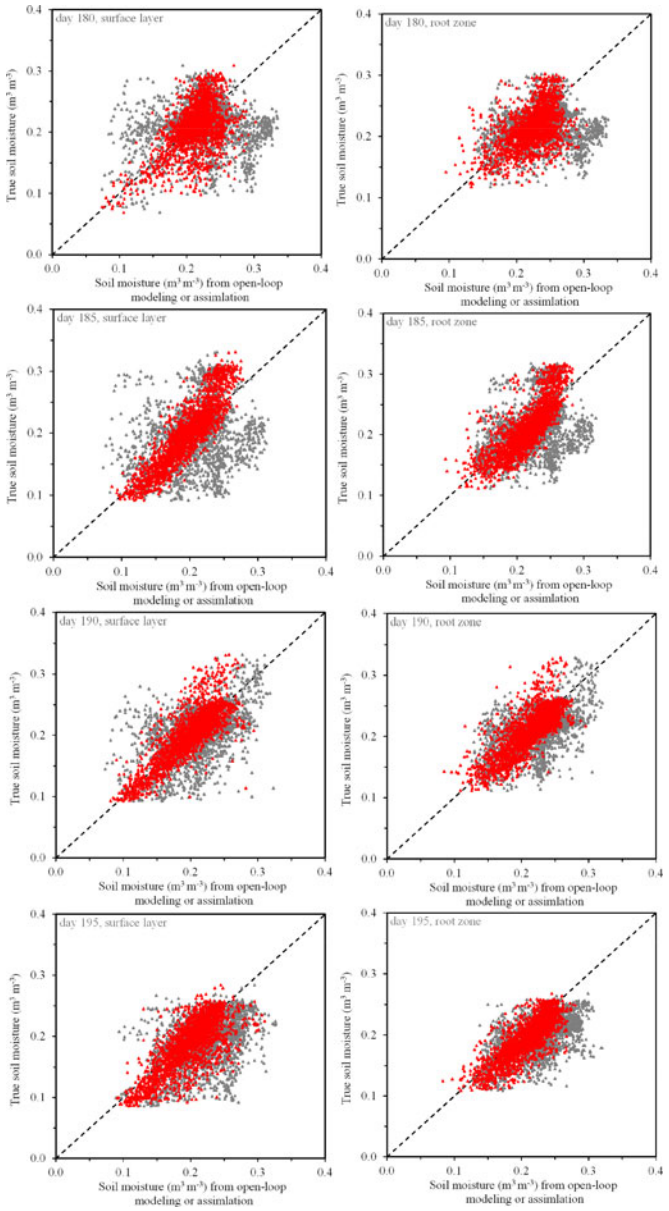

Fig. 4. Scatterplot of soil moisture estimates for (left) the surface layer and (right) root zone on (top to bottom) days 180, 185, 190, and 195, respectively: (symbols in gray) open-loop model versus the reference solution ("truth"), and (symbols in red) assimilation versus "truth." The dashed line is the one-to-one line.

"true" state and to assimilate soil moisture retrievals. In practice, it may be challenging to improve soil moisture estimates for root zone due to a lack of perfect forecast models and complete knowledge of the satellite observation errors.

The statistical analyses of the soil moisture spatial pattern are presented in Figs. 4 and 5. For either the surface layer or root-zone soil moisture estimates across the study domain, the bias between the open-loop model and "truth" is typically larger than that between the assimilation estimation and "truth." The soil moisture estimates from the assimilation, relative to the open-loop estimates, exhibit a higher correlation with the truth, especially in summer days.

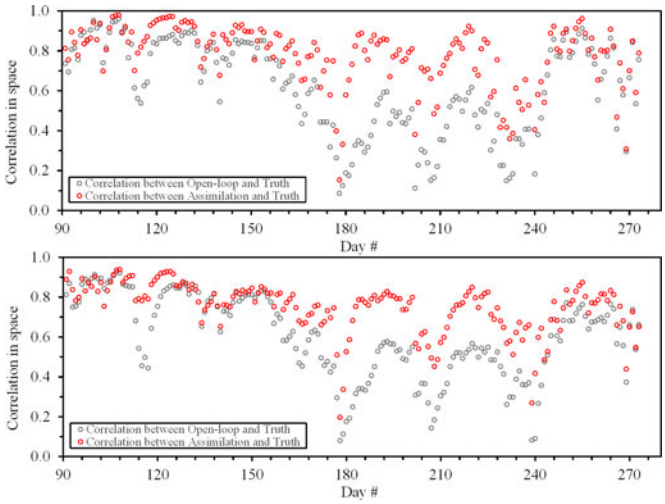

Fig. 5. Temporal variation of correlation in space of soil moisture estimates from (gray symbols) the open-loop model and (red symbols) the assimilation against "truth." (top) the surface layer and (bottom) root zone.

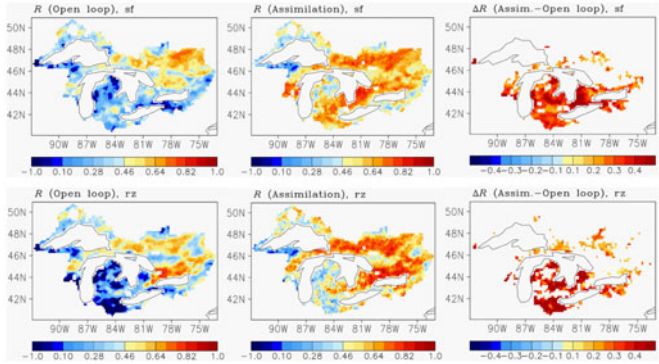

Fig. 6. Soil moisture skill R from (left) the open-loop model and (middle) the assimilation, and (right) the skill improvement ΔR (assimilation minus open loop) for (top) the surface layer (0–10 cm) and (bottom) root zone (0–35 cm). ΔR is displayed only when the open-loop R and the assimilation R are significantly (5% level) different from each other.

In practice, *in situ* soil moisture measurements, which serve as the "ground truth," are typically based upon sparse point sources. Point-scale measurements, due to the sampling error, are usually difficult to represent the areal average (satellite or model estimates) in terms of the absolute magnitude of soil moisture [33], [34]. In contrast, the temporal variability of soil moisture observed by point measurements are spatially representative [35]–[37]. On the other hand, in reality, due to the satellite-model bias (systematic error), satellite retrievals usually need to be rescaled (locally) prior to data assimilation [38]. Since the absolute magnitude of satellite soil moisture is locally changed the absolute values and the spatial pattern of the assimilation estimation are meaningless. Instead, the assimilation products are more meaningful in terms of the time variability of soil moisture, which is consistent with the advantage of point measurements. Hence, the time-series correlation R metric, relative to the spatial analysis and the root-mean-square error (RMSE), is more appropriate for a quantitative assessment of the assimilation performance in practical applications.

To be consistent with real applications, here we focus upon the soil moisture skill R metric, which is defined as the daily time-series correlation of soil moisture estimates (satellite data, open-loop model, or assimilation estimates) with the "true" soil moisture solution. We compute the R values using data between 1 April and 30 September since for our study domain, in practice, the effects of snow cover and frozen soils are the weakest on satellite soil moisture estimates during this period. We also calculated the RMSE results (not presented here), which did not change our general conclusions based on the R measure. This is not surprising since the correlation R metric is as informative as the RMSE metric [39].

Fig. 6 compares the skill R values from the open-loop and the assimilation estimates for both surface and root-zone soil moisture across the study domain. The Fisher Z transform method [40], [41] is used to test the significance of the skill improvement ΔR, defined as the skill for the assimilation product minus the skill for the open-loop estimates (see Fig. 6, right). Overall, either the open-loop model or the assimilation provides similar spatial pattern of skill for surface (see Fig. 6, top) and root-zone soil moisture (see Fig. 6, bottom). The open-loop model (see Fig. 6, left) typically provides lower soil moisture skill R at the grids dominated by crop cover (mean of 0.29 (0.16) for surface (root zone)) than for forest-dominated grids (mean of 0.41(0.42) for surface (root zone)) (the vegetation cover distribution is shown in Fig. 1). This is not surprising because the seasonal variations in canopy, in terms of a growth index, are treated differently between trees and crops in the MESH model. For all vegetation types, the growth index is set to 1 for fully leafed periods, to 0 for leafless periods, and to be linear during the transition periods. For trees, the transition periods are determined by the surface air temperature and the surface soil temperature; while the transition periods of crops are specified using certain days based upon their latitudes [42]. Through data assimilation, almost all grids experience positive skill gains but with different magnitudes. In general, the skill improvement ΔR decreases with increased open-loop skill, coinciding with the finding of [43]. The strong and statistically significant skill improvements are typically observed for crop-dominated grids.

B. Impact of Ensemble Size

To perform the EnKF assimilation, the ensemble size N and the radius of influence for the observations r need to be appropriately configured. Throughout this study, r is zero since the 1D-EnKF is used (i.e., for a given observation, the analysis update (2) is only applied to state variables at the observation location). In experiment A, an ensemble of 12 members are used. To assess the impact of ensemble size, we repeat experiment A with $N = 6$ (experiment B1), 50 (experiment B2), and 100 (experiment B3), respectively. The mean soil moisture skill results from these experiments are summarized in Fig. 7. The soil moisture skill values from experiment B1 ($N = 6$) are slightly reduced from those obtained in experiment A ($N = 12$). On the other hand, increasing N to 50 or 100 has smaller (but opposite) effects. Such dependence on N is also consistent with other studies [44], [45].

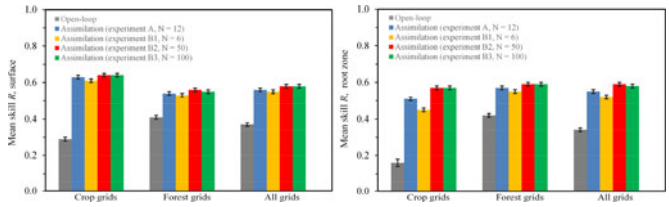

Fig. 7. Averaged soil moisture skill R for the open-loop model and the assimilation estimates from experiments A, B1, B2, and B3 (see Table I for key): (left) Surface layer (top 10 cm) and (right) root zone (top 35 cm). The (area averaged) R values are computed, respectively, for the crop-dominated grids, the forest-dominated grids, and all model grids (except for water and impervious surfaces) within the study domain. Error bars indicate 95% confidence intervals.

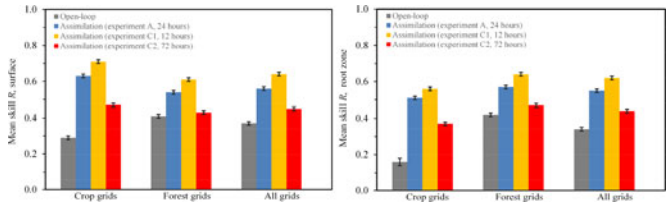

Fig. 8. Similar to Fig. 7, except that the assimilation estimates are from experiments A, C1, and C2 (see Table I for key), respectively.

Overall, a small ensemble size is generally sufficient for the 1D-EnKF to perform well in land surface/hydrological models that typically, in contrast to atmospheric models, do not involve chaotic processes. Furthermore, the analysis increment calculations in the 1D-EnKF are conducted independently for the model grids (horizontal correlations are neglected) and the state vector is, thus, relatively small in dimension. An increased ensemble size would be required if horizontal correlations are taken into account (i.e., a 3D EnKF) [46]. Additionally, note that a larger ensemble size would clearly be of advantage for suppressing statistical noise in error covariance estimates of the state variables and in error correlations between the states and the measured variable [44]. This may explain the more satisfactory assimilation estimates of root-zone soil moisture in cropped areas when the ensemble size is increased to 50 or 100 (see Fig. 7, right).

C. *Effect of Observing Frequency*

In reality, soil moisture retrievals derived from satellite microwave sensors (except for synthetic aperture radars) typically have a time resolution of 1–3 days (separately for the ascending and descending overpasses). Experiments C1 and C2 are designed to evaluate the impact of the frequency of the satellite observations on the assimilation estimates. Experiment C1 (C2) is the same as experiment A, except for assimilating the synthetic retrievals at 12-h (72-h) intervals. Fig. 8 presents the mean soil moisture skill from experiments A, C1, and C2. Clearly, the soil moisture estimates can be further enhanced (experiment C1) when the satellite observations are assimilated more frequently (i.e., a shorter assimilation interval). In contrast, a longer assimilation interval (experiment C2) decreases the skill improvement obtained by data assimilation. Inclusion of more observational information would clearly be of advantage. Therefore, in practice, to produce the best soil moisture estimates, we should jointly assimilate the retrievals from both ascending and descending orbits or from different platforms. A joint assimilation of the Advanced Microwave Scanning Radiometer-Earth Observing System (AMSR-E) and the Advanced Scatterometer (ASCAT) soil moisture retrievals into the NASA catchment land surface model could lead to higher soil moisture skill (anomaly R) than the alone assimilation of either of the two retrieval datasets [20].

Note that the "best" assimilation estimates resulting from experiment C1 were based upon the synthetic retrievals with the same accuracy. In [20], the two sensor products (AMSR-E and ASCAT) also had similar retrieval skills, and, therefore, their joint assimilation was promising. In practice, however, the retrievals derived from different orbits (ascending or descending) or from different sensors may have different accuracies. For example, L-band sensors (e.g., the Microwave imaging radiometer with aperture synthesis onboard the soil moisture and ocean salinity (SMOS) mission) are expected to provide better soil moisture estimates than the sensors operating at X or C bands (e.g., AMSR-E) since the latter (operating at shorter bands) are more susceptible to vegetation effects. Such discrepancies could impact the performance of their joint assimilation, i.e., a joint assimilation of soil moisture retrieval datasets from different sensor systems (at different overpassing times), although it means a shorter assimilation interval or an increased observing frequency (such as in experiment C1) does not necessarily yield the "best" skill. To demonstrate this point, we also performed an additional experiment in which we jointly assimilated two synthetic retrieval datasets with different accuracies. The first retrieval dataset is same as that used in experiment A (the synthetic retrievals were obtained once daily from the truth soil moisture by adding white noise with a standard deviation of $0.08\,m^3/m^3$). The second retrieval dataset is generated once daily (measurement time is shifted by 12 h relative to the first dataset to represent a different sensor overpassing time) by applying the noise standard deviations of $0.12\,m^3/m^3$ to the truth soil moisture. The mean (basin-averaged) retrieval skill (correlation R between synthetic retrievals and the truth fields) for the first and second retrieval datasets, and their combination are 0.60, 0.44, and 0.54, respectively. The second retrieval dataset is then assimilated (alone and jointly with the first retrieval dataset, respectively) into the model. Note that a true observation error standard deviation (0.08 and $0.12\,m^3/m^3$ for the two retrieval datasets, respectively) is always used for the alone or joint assimilation experiments. Results (not shown here) suggest that the soil moisture skill R from the joint assimilation (12-h intervals) is higher than that when assimilating the second retrieval dataset alone (24-h intervals), but is lower than that from experiment A (24-h intervals). This confirms that a joint assimilation of different retrieval datasets does not necessarily yield the "best" estimation. Note that the combined retrieval set (twice daily) has a different retrieval skill from either the first or second retrieval set (once daily), although the influence of retrieval skill (see a comparison of experiments A, D1, and D2 presented in Fig. 9) is a consistent explanation for the observing frequency modulation on the assimilation skill.

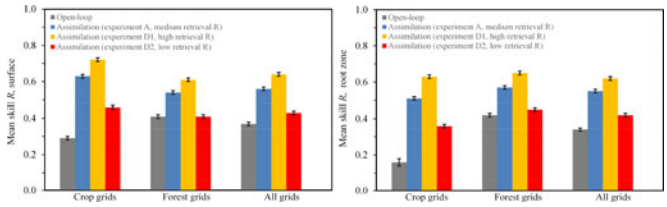

Fig. 9. Similar to Fig. 7, except that the assimilation estimates are from experiments A, D1, and D2 (see Table I for key), respectively.

D. Impact of Retrieval Skill

In practice, the soil moisture retrievals derived from different sensor systems typically have different accuracies. In experiment A, the synthetic satellite retrievals (daily-spaced) were generated by applying the white noise with a standard deviation of 0.08 m^3/m^3 to the true soil moisture. The resulting retrieval dataset has a mean (basin-averaged) retrieval skill of about 0.60. To mimic the desired retrieval accuracy for SMOS [10] and SMAP missions [11] and other retrieval errors, here we change the random errors applied to the synthetic satellite soil moisture retrievals. By applying the noise with standard deviations of 0.04 and 0.12 m^3/m^3, separately, to the "true" soil moisture, two additional synthetic retrieval datasets (daily-spaced), with mean retrieval skill of 0.74 and 0.43, respectively, are produced, and are subsequently assimilated into the model (experiments D1 and D2). Still a true observation error standard deviation is used for the synthetic assimilation (0.04 and 0.12 m^3/m^3 for D1 and D2, respectively). Fig. 9 compares the mean soil moisture skill results from experiments A, D1, and D2. Clearly, the three synthetic retrieval datasets lead to three sets of assimilation estimates with different accuracies. Relative to experiment A, the mean soil moisture skill is further improved in experiment D1, but is degraded in experiment D2. This demonstrates that the skill improvement increases with increasing retrieval skill.

E. Sensitivity to Input Error Parameters

In experiment A, as mentioned earlier, the model input error parameters (see Table II) were specified, and a true observation error standard deviation was used for the synthetic retrievals. Now, we test the impact of the specified model and observation input error parameters through a group of new experiments. For the new experiments, the truth solution and synthetic satellite retrievals are different from those used in experiment A. Following [32], the truth and synthetic satellite retrievals are generated as follows (see Fig. 10). First, we integrate the MESH model from 1 January to 31 December with the 2006 forcing data (the model is spun up by a ten-year repeated simulation using the 2005 forcings). The resulting soil moisture serves as the unperturbed "open-loop" solution. Next, using the same forcing data and for the same period, we perform the MESH model ensemble simulations (12 members) with the error perturbation parameters listed in Table II. We randomly select an ensemble member integration to serve as the synthetic "truth" (so that the perturbation parameters listed in Table II serve as the "truth" model error inputs). For a given grid, the synthetic satellite soil moisture retrievals are generated by adding the white noise with a standard deviation of 0.05 m^3/m^3 to the surface soil moisture estimates that are extracted from the "true" fields at 24-h intervals. Finally, the synthetic retrievals are assimilated into the MESH model with the 1D-EnKF scheme. The assimilation will be repeatedly conducted using different sets of error perturbation parameters to explore the impact of input error parameters.

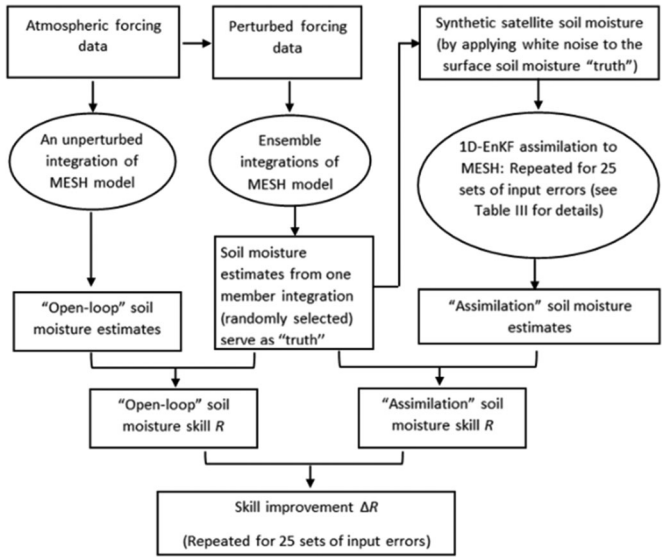

Fig. 10. Flowchart of the assimilation experiments to identify the impact of input error parameters

TABLE III
INPUT ERROR OR PARAMETERS (UNIT: m^3m^{-3}) FOR EXPERIMENTS E1–E25

Observation error stdev	Error stdev for the modeled volumetric liquid water in the three soil layers				
	2.E−04; 1.E−04; 2.E−06	5.E−04; 2.E−04; 1.E−05	1.E−03; 5.E−04; 5.E−05	2.E−03; 1.E−03; 1.E−04	4.E−03; 2.E−03; 2.E−04
0.005	E1	E2	E3	E4	E5
0.02	E6	E7	E8	E9	E10
0.05	E11	E12	E13[a]	E14	E15
0.08	E16	E17	E18	E19	E20
0.11	E21	E22	E23	E24	E25

[a]The reference ("truth") model and observation input error parameters are used.

Here, we choose five sets of input model error parameters, which approximately represent five different forecast error stand deviations (stdev) and five values of observation error stdev (see Table III). Each of the five sets of input model error parameters and each observation error standard deviation are grouped together for use in the assimilation integrations. We do not change the forcing perturbations and the model error correlation time, which are still same as those listed in Table II. Therefore, we can perform 25 assimilation experiments (E1 to E25). Note that one of the 25 experiments (see E13 in Table III) uses the reference ("truth") model and observation error inputs.

Based upon the E1 to E25 results, we can plot the assimilation performance, in terms of the (study domain-averaged) soil moisture skill improvement (assimilation—open loop), as a function

TABLE IV
BASIN-AVERAGED ANOMALY *R* FOR SOIL MOISTURE ESTIMATES

Soil moisture estimates[a]	Mean anomaly *R* with 95% confidence intervals	
	Surface layer	Root zone
Open-loop	0.14 ± 0.01	0.14 ± 0.01
Assimilation (Exp. A)	0.40 ± 0.01	0.39 ± 0.01
Assimilation (Exp. B1)	0.38 ± 0.01	0.35 ± 0.01
Assimilation (Exp. B2)	0.41 ± 0.01	0.42 ± 0.01
Assimilation (Exp. B3)	0.40 ± 0.01	0.41 ± 0.01
Assimilation (Exp. C1)	0.49 ± 0.01	0.47 ± 0.01
Assimilation (Exp. C2)	0.26 ± 0.01	0.26 ± 0.01
Assimilation (Exp. D1)	0.49 ± 0.01	0.48 ± 0.01
Assimilation (Exp. D2)	0.25 ± 0.01	0.24 ± 0.01

[a]See Table I for experimental key.

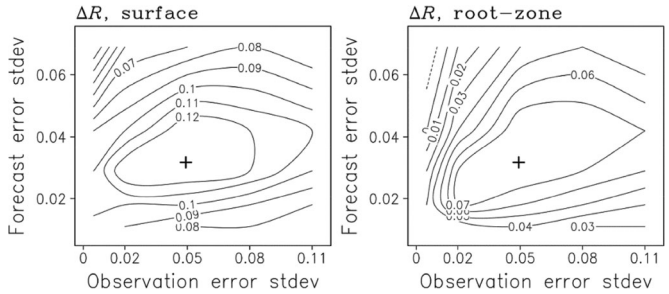

Fig. 11. Skill improvement ΔR (assimilation—open loop) for (left) surface and (right) root-zone soil moisture as a function of the forecast and observation error standard deviations (stdev, units: m^3m^{-3}). The plus sign denotes the assimilation experiment with the "true" model and observation error inputs.

of the (study domain and time averaged) forecast and observation error standard deviations (see Fig. 11). As expected, the skill improvement ΔR in both surface and root-zone soil moisture is the strongest when the input error parameters are close to their true values (plus signs). Overall, when the input error parameters are wrongly specified (i.e., deviating from their true values) the EnKF filter assimilation still produces an increased skill (i.e., a positive ΔR), although the skill improvement ΔR will be decreased. However, if a severe underestimation of observation error occurs, the skill improvement ΔR, especially for root-zone soil moisture, could be very weak or even negative (i.e., the assimilation estimates are worse than the open loop). This illustrates that even without online (adaptive) tuning of the observation and model error parameters the EnKF filter is typically able to improve soil moisture estimates as long as the observation errors are not severely underestimated. Similar performance may be also applicable to the assimilation estimates of runoff (e.g., [47]).

V. SUMMARY AND DISCUSSION

In this study, we presented the implementation of the 1D-EnKF scheme to assimilate satellite soil moisture into the standalone version of the MESH model. To examine the performance of the established assimilation scheme under different conditions, we have conducted a series of synthetic assimilation experiments. The experiments demonstrated the capability of the assimilation system to accurately approximate the "true" surface and root-zone soil moisture states given satellite observations and the intentionally degraded model estimates. Through assimilation of satellite soil moisture, almost all areas experienced positive skill gains ΔR (assimilation—open loop) but typically with stronger and statistically significant ΔR for the cropped grids, which generally exhibited low open-loop skill.

A small ensemble size is generally sufficient for the 1D-EnKF to perform well because the analysis increment calculations are conducted independently for the model grids (horizontal correlations are neglected). An increased observing frequency (i.e., a shorter assimilation interval) typically can further enhance the assimilation estimates. Therefore, in any practical application, to produce the best estimates, we should jointly assimilate the retrievals from all the available sources. However, note that a joint assimilation (i.e., an increased observing frequency) of the retrieval sets with significantly different observation skills does not necessarily yield the "best" estimation. The skill improvement typically increases with the increasing retrieval skill. Even without online (adaptive) tuning of the observation and model error parameters, the skill of the assimilation product typically exceeds the skill of the open-loop model (i.e., a positive ΔR) except when the observation errors are severely underestimated. The findings have provided an important guidance for the practical applications of the assimilation scheme [48], [49].

The skill *R* values presented in this study are derived based upon the raw soil moisture time series. To evaluate the impact of soil moisture seasonality on the skill *R* estimation, we also computed the anomaly correlation *R* for the open-loop modeling and the assimilation from experiments A to D2 (see Table IV). The soil moisture anomalies are defined as departures of daily soil moisture from the monthly mean. Overall the raw *R* metric of skill and the anomaly *R* metric lead to the consistent general conclusions.

Note that, in practice, the assimilation of satellite soil moisture will encounter a number of critical challenges, which were avoided in our synthetic experiments. They mainly include: 1) the model-satellite measurement scale discrepancy. Soil moisture derived from spaceborne passive microwave measurements typically have relatively coarse spatial resolution, whereas there is an increased demand for conducting land/hydrologic simulations at high spatial resolution. This raises a question: how to integrate coarse-scale satellite products and fine-scale land/hydrologic models. For the 1D-EnKF assimilation, *a priori* disaggregation (downscaled) scheme is typically used, i.e., coarse resolution observations are disaggregated and remapped onto the model grids prior to assimilation. For the 3D-EnKF filter (i.e., horizontal correlations between model grids are considered), we may conduct a direct assimilation of coarse-scale satellite products by upscaling the model forecast. 2) Statistical bias between satellite and model soil moisture estimates. In practice, satellite-based soil moisture and model estimates typically exhibit different climatologies, which will violate the hypothesis of unbiased errors in model and observation (for a bias-blind assimilation system). To reduce or remove the satellite-model bias, *a priori* observation rescaling by matching the cumulative distribution functions of the two datasets is often practical [38]. *A priori* calibration of the model

with the climatology of satellite soil moisture can also be used to remove the bias [50]. 3) Difficulty in quantifying satellite observation errors. The synthetic experiments indicate that the accurate specification of observation error covariance is crucial to the success of the analysis. Satellite soil moisture retrievals are typically subject to both instrumental errors and representativeness errors. The latter are caused primarily by the observation operator used in the retrieval algorithm and the misfit between the observation space and the model space. In reality, the errors in satellite retrievals, especially the representativeness errors, are difficult or impossible to completely estimate since they highly vary with time and space. Some approximations could be efficient. For example, the satellite product climatology can approximately serve as the observation errors [19], [20].

ACKNOWLEDGMENT

The authors would like to thank A. Haghnegahdar for providing the calibrated MESH model parameter set. They would also like to thank the two anonymous reviewers for their helpful comments on the original paper.

REFERENCES

[1] C. M. Taylor, R. A. M. de Jeu, F. Guichard, P. P. Harris, and W. A. Dorigo, "Afternoon rain more likely over drier soils," *Nature*, vol. 489, pp. 423–426, Sep. 2012.

[2] T. W. Collow, A. Robock, and W. Wu, "Influences of soil moisture and vegetation on convective precipitation forecasts over the United States great plains," *J. Geophys. Res. Atmos.*, vol. 119, no. 15, pp. 9338–9358, Aug. 2014.

[3] E. P. Maurer and D. P. Lettenmaier, "Predictability of seasonal runoff in the mississippi river basin," *J. Geophys. Res.*, vol. 108, no. D16, p. 8607, Aug. 2003.

[4] W. R. Atlas and Y. C. Sud, "Numerical experiments related to the summer 1980 US heat wave," *Monthly Weather Rev.*, vol. 115, no. 8, pp. 1345–1357, Jul. 1987.

[5] E. M. Fischer, S. I. Seneviratne, P. L. Vidale, D. Luthi, and C. Schar, "Soil moisture-atmosphere interactions during the 2003 European summer heat wave," *J. Clim.*, vol. 20, no. 20, pp. 5081–5099, Oct. 2007.

[6] T. J. Jackson, "Soil moisture estimation using special satellite microwave/imager satellite data over a grassland region," *Water Resour. Res.*, vol. 33, no. 6, pp. 1475–1484, Jun.1997.

[7] R. Bindlish *et al.*, "Soil moisture estimates from TRMM microwave imager observations over the Southern United States," *Remote Sens. Environ.*, vol. 85, no. 4, pp. 507–515, Jun. 2003.

[8] E. G. Njoku, T. J. Jackson, V. Lakshimi, Y. K. Chan, and S. V. Nghiem, "Soil moisture retrieval from AMSR-E," *IEEE Trans. Geosci. Remote Sens.*, vol. 41, no. 2, pp. 215–229, Feb. 2003.

[9] M. Owe, R. A. M. de Jeu, and T. H. R. Holmes, "Multisensor historical climatology of satellite-derived global land surface soil moisture," *J. Geophys. Res.*, vol. 113, no. F1, p. F01002, Mar. 2008.

[10] Y. H. Kerr, P. Waldteufel, J. P. Wigneron, J. M. Martinuzzi, J. Font, and M. Berger, "Soil moisture retrieval from space: The soil moisture and ocean salinity (SMOS) mission," *IEEE Trans. Geosci. Remote Sens.*, vol. 39, no. 8, pp. 1729–1735, Aug. 2001.

[11] D. Entekhabi *et al.*, "The soil moisture active and passive (SMAP) mission," *Proc. IEEE*, vol. 98, no. 5, pp. 704–716, May 2010.

[12] L. Brocca, F. Ponziani, T. Moramarco, F. Melone, N. Berni, and W. Wagner, "Improving landslide forecasting using ASCAT-derived soil moisture data: A case study of the Torgiovannetto landslide in central Italy," *Remote Sens.*, vol. 4, no. 5, pp. 1232–1244, May 2012.

[13] W. Wagner *et al.*, "The ASCAT soil moisture product: A review of its specifications, validation results, and emerging applications," *Meteorologische Zeitschrift*, vol. 22, no. 1, pp. 5–33, Feb. 2013.

[14] T. E. Ochsner *et al.*, "State of the art in large-scale soil moisture monitoring," *Soil Sci. Soc. Amer. J.*, vol. 77, no. 6, pp. 1888–1919, Oct. 2013.

[15] R. H. Reichle, "Data assimilation methods in the earth sciences," *Adv. Water Resour.*, vol. 31, pp. 1411–1418, Jan. 2008.

[16] X. Xu, J. Li, and B. A. Tolson, "Progress in integrating remote sensing data and hydrologic modeling," *Prog. Phys. Geogr.*, vol. 38, no. 4, pp. 464–498, Aug. 2014.

[17] R. H. Reichle and R. D. Koster, "Global assimilation of satellite surface soil moisture retrievals into the NASA Catchment land surface model," *Geophys. Res. Lett.*, vol. 32, p. L02404, Jan. 2005.

[18] R. H. Reichle, R. D. Koster, P. Liu, S. P. P. Mahanama, E. G. Njoku, and M. Owe, "Comparison and assimilation of global soil moisture retrievals from the advanced microwave scanning radiometer for the earth observing system (AMSR-E) and the scanning multichannel microwave radiometer (SMMR)," *J. Geophys. Res.*, vol. 112, no. D9, p. D09108, May 2007.

[19] Q. Liu *et al.*, "The contributions of precipitation and soil moisture observations to the skill of soil moisture estimates in a land data assimilation system," *J. Hydrometeorol.*, vol. 12, no. 5, pp. 750–765, Oct. 2011.

[20] C. S. Draper, R. H. Reichle, G. J. M. De Lannoy, and Q. Liu, "Assimilation of passive and active microwave soil moisture retrievals," *Geophys. Res. Lett.*, vol. 39, no. 4, p. L04401, Feb. 2012.

[21] L. Zhao *et al.*, "The scale-dependence of SMOS soil moisture accuracy and its improvement through land data assimilation in the central Tibetan Plateau," *Remote Sens. Environ.*, vol. 152, pp. 345–355, Sep. 2014.

[22] C. Francois, A. Quesney, and C. Ottle, "Sequential assimilation of ERS-1 SAR data into a coupled land surface–hydrological model using an extended Kalman filter," *J. Hydrometeorol.*, vol. 4, no. 2, pp. 473–487, Apr. 2003.

[23] J. M. Jacobs, D. A. Meyers, and B. M. Whitfield, "Improved rainfall/runoff estimates using remotely-sensed soil moisture," *J. Amer. Water Resour. Assoc.*, vol. 39, no. 2, pp. 313–324, Apr. 2003.

[24] A. Pietroniro *et al.*, "Development of the MESH modelling system for hydrological ensemble forecasting of the Laurentian Great Lakes at the regional scale," *Hydrol. Earth Syst. Sci.*, vol. 11, no. 4, pp. 1279–1294, May 2007.

[25] N. Kouwen, E. D. Soulis, A. Pietroniro, J. Donald, and R. A. Harrington, "Grouped response units for distributed hydrologic modelling," *J. Water Resour. Plan. Manage.*, vol. 119, no. 3, pp. 289–305, Jun. 1993.

[26] W. A. Flügel, "Delineating hydrological response units by geographical information system analyses for regional hydrological modelling using PRMS/MMS in the drainage basin of the River Bröl, Germany," *Hydrological Processes*, vol. 9, nos. 3/4, pp. 423–436, Apr./May 1995.

[27] W. A. Flügel, M. Märker, S. Moretti, G. Rodolfi, and A. Sidrochuk, "Integrating geographical information systems, remote sensing, ground truthing and modelling approaches for regional erosion classification of semi-arid catchments in South Africa," *Hydrological Processes*, vol. 17, no. 5, pp. 929–942, Mar. 2003.

[28] S. J. Park and N. van de Giesen, "Soil-landscape delineation to define spatial sampling domains for hillslope hydrology," *J. Hydrol.*, vol. 295, nos. 1–4, pp. 28–46, Aug. 2004.

[29] A. Haghnegahdar *et al.*, "Calibrating Environment Canada's MESH modelling system over the Great Lakes basin," *Atmos. Ocean*, vol. 52, no. 4, pp. 281–293, Aug. 2014.

[30] G. Evensen, "Sequential data assimilation with a non-linear quasi-geostrophic model using Monte-Carlo methods to forecast error statistics," *J. Geophys. Res.*, vol. 99, no. C5, pp. 10143–10162, May 1994.

[31] J. Mailhot *et al.*, "The 15-km version of the Canadian regional forecast system," *Atmos. Ocean*, vol. 44, no. 2, pp. 133–149, Nov. 2006.

[32] R. H. Reichle, W. T. Crow, and C. L. Keppenne, "An adaptive ensemble Kalman filter for soil moisture data assimilation," *Water Resour. Res.*, vol. 44, no. 3, p. W03423, Mar. 2008.

[33] T. J. Jackson *et al.*, "Validation of advanced microwave scanning radiometer soil moisture products," *IEEE Trans. Geosci. Remote Sens.*, vol. 48, no. 12, pp. 4256–4272, Dec. 2010.

[34] W. T. Crow *et al.*, "Upscaling sparse ground-based soil moisture observations for the validation of coarse-resolution satellite soil moisture products," *Rev. Geophys.*, vol. 50, no. 2, Jun. 2012.

[35] L. Brocca, F. Melone, T. Moramarco, and R. Morbidelli, "Soil moisture temporal stability over experimental areas in Central Italy," *Geoderma*, vol. 148, nos. 3/4, pp. 364–374, Jan. 2009.

[36] A. Loew and W. Mauser, "On the disaggregation of passive microwave soil moisture data using a priori knowledge of temporally persistent soil moisture fields," *IEEE Trans. Geosci. Remote Sens.*, vol. 46, no. 3, pp. 819–834, Mar. 2008.

[37] J. Martinez-Fernandez and A. Ceballos, "Mean soil moisture estimation using temporal stability analysis," *J. Hydrol.*, vol. 312, nos. 1–4, pp. 28–38, Oct. 2005.

[38] R. H. Reichle and R. D. Koster, "Bias reduction in short records of satellite soil moisture," *Geophys. Res. Lett.*, vol. 31, no. 19, p. L19501, Oct. 2004.
[39] D. Entekhabi, R. H. Reichle, R. D. Koster, and W. T. Crow, "Performance metrics for soil moisture retrievals and application requirements," *J. Hydrometeorol.*, vol. 11, no. 3, pp. 832–840, Jun. 2010.
[40] O. J. Dunn and V. Clark, "Correlation coefficients measured on the same individuals," *J. Amer. Statis. Assoc.*, vol. 64, no. 325, pp. 366–377, Mar. 1969.
[41] X. Meng, R. Rosenthal, and D. B. Rubin, "Comparing correlated correlation coefficients," *Psychol. Bull.*, vol. 111, no. 1, pp. 172–175, Jan. 1992.
[42] D. L. Verseghy, N. A. McFarlane, and M. Lazare, "Class—A Canadian land surface scheme for GCMS. II. Vegetation model and coupled runs," *Int. J. Climatol.*, vol. 13, no. 4, pp. 347–370, May 1993.
[43] R. H. Reichle, W. T. Crow, R. D. Koster, H. O. Sharif, and S. P. P. Mahanama, "Contribution of soil moisture retrievals to land data assimilation products," *Geophys. Res. Lett.*, vol. 35, no. 1, p. L01404, Jan. 2008.
[44] R. H. Reichle, J. P. Walker, R. D. Koster, and P. R. Houser, "Extended versus ensemble Kalman filtering for land data assimilation," *J. Hydrometeorol.*, vol. 3, no. 6, pp. 728–740, Dec. 2002.
[45] J. Yin, X. Zhan, Y. Zheng, C. R. Hain, J. Liu, and L. Fang, "Optimal ensemble size of ensemble Kalman filter in sequential soil moisture data assimilation," *Geophys. Res. Lett.*, vol. 42, no. 16, pp. 6710–6715, Aug. 2015.
[46] R. H. Reichle, D. B. McLaughlin, and D. Entekhabi, "Hydrologic data assimilation with the ensemble Kalman filter," *Monthly Weather Rev.*, vol. 130, no. 1, pp. 103–114, Jan. 2002.
[47] C. Massari, L. Brocca, A. Tarpanelli, and T. Moramarco, "Data assimilation of satellite soil moisture into rainfall-runoff modelling: A complex recipe?" *Remote Sens.*, vol. 7, pp. 11403–11433, Sep. 2015.
[48] X. Xu *et al.*, "Assimilation of SMOS soil moisture in the MESH model with the ensemble Kalman filter," in *Proc. IEEE Int. Geosci. Remote Sens. Symp.*, Jul. 2014, pp. 3766–3769.
[49] X. Xu *et al.*, "Assimilation of SMOS soil moisture over the Great Lakes basin," *Remote Sens. Environ.*, vol. 169, pp. 163–175, Nov. 2015.
[50] S. V. Kumar, R. H. Reichle, K. W. Harrison, C. D. Peters-Lidard, S. Yatheendradas, and J. A. Santanello, "A comparison of methods for a priori bias correction in soil moisture data assimilation," *Water Resour. Res.*, vol. 48, no. 3, p. W03515, Mar. 2012.

Xiaoyong Xu received the B.Sc. and M.Sc. degrees in atmospheric physics from Nanjing Institute of Meteorology, Nanjing, China, in 1999 and 2002, respectively, and the Ph.D. degree in geography from the University of Waterloo, Waterloo, ON, Canada, in 2015.

He was a Research Associate with the NOAA National Severe Storms Laboratory and the Cooperative Institute for Mesoscale Meteorological Studies, University of Oklahoma, Norman, USA, in 2006–2007. From 2007 to 2011, he was a CANDAC Research Fellow with the University of Saskatchewan, Saskatoon, Canada. He is currently a Postdoctoral Scientist at Aquanty Inc., Waterloo. His broad research interests include hydrological and atmospheric sciences, including hydrologic remote sensing, land data assimilation, atmospheric coupling processes, and radar data assimilation.

Bryan A. Tolson received the B.Sc. degree in environmental science from the University of Guelph, Guelph, ON, Canada, in 1998, the M.A.Sc. degree in civil engineering from the University of British Columbia, Vancouver, BC, Canada, in 2000, and the Ph.D. degree in civil and environmental engineering from Cornell University, Ithaca, NY, USA, in 2005.

Since 2012, he has been an Associate Professor in the Department of Civil and Environmental Engineering, University of Waterloo, Waterloo, ON, where from 2005 to 2012, he was an Assistant Professor. His research interests include environmental and water resources systems analysis, the development and testing of heuristic algorithms for efficient single- and multiple-objective optimization, and uncertainty estimation, as well as risk-based or probabilistic assessment of environmental and water resources systems.

Jonathan Li (M'00–SM'11) received the Ph.D. degree in geomatics engineering from the University of Cape Town, Cape Town, South Africa, in 2000.

He is currently a Professor in the Department of Geography and Environmental Management, University of Waterloo, Waterloo, ON, Canada. He is the coauthor of more than 300 publications, more than 150 of which are refereed journal papers, including the *Remote Sensing of the Environment*, the IEEE TRANSACTIONS ON GEOSCIENCE AND REMOTE SENSING, and the IEEE JOURNAL OF SELECTED TOPICS IN APPLIED EARTH OBSERVATIONS AND REMOTE SENSING. His research interests include geometric and semantic information extraction from earth observation data and mobile laser scanning data.

Dr. Li is an Associate Editor of the IEEE TRANSACTIONS ON INTELLIGENT TRANSPORTATION SYSTEMS and the IEEE JOURNAL OF SELECTED TOPICS IN APPLIED EARTH OBSERVATIONS AND REMOTE SENSING.

Bruce Davison was born in London, England, U.K., in 1975. He received the B.Sc. degree in systems design engineering and the M.Sc. degree in civil engineering from the University of Waterloo, Waterloo, ON, Canada, in 2000 and 2004, respectively, and the Ph.D. degree in atmospheric and oceanic sciences from McGill University, Montréal, QC, Canada, in 2016.

Since 2004, he has been with Environment Canada, Saskatoon, SK, Canada, as a Hydrologist. His primary research interests include hydrometeorological modeling, including incorporating physical or statistical processes into models, operationalization of modelling tools, incorporating software engineering tools into model development, and models used for decision making.

Mr. Davison is a Professional Engineer with the Association of Professional Engineers and Geoscientists of Saskatchewan and a Member of the Canadian Geophysical Union, the Canadian Water Resources Association, and the Canadian Meteorological and Oceanographic Society.